
Michael Schmutz

# Seasonal and inter-annual variation of $CO_2$ flux and $CO_2$ concentration in Basel

M. Schmutz[1], R. Vogt[1], E. Parlow[1]

[1] *University of Basel, Research Group for Meteorology, Climate and Remote Sensing, Klingelbergstrasse 27, 4056 Basel, mi.schmutz@unibas.ch*

dated : 15 May 2015

## 1. Introduction

Measurements of flux ($F_c$) and concentration ($\rho_c$) of carbon dioxide ($CO_2$) are carried out in different ecosystems since several decades. Nevertheless, multiyear records in the urban environment are rare and, when available, cover at most a few years. In Basel, Switzerland, $F_c$ and $\rho_c$ are measured continuously since May 2004 by an eddy covariance system at 38 m above street level at Klingelbergstrasse (BKLI) covering in the meantime a full decade. Analysis of this unique time series contributes to an enhanced understanding of controlling factors of $\rho_c$ and $F_c$ as well as their seasonal and inter-annual variation in the urban environment.

## 2. Study Site

Long-term urban meteorological measurements are carried out by the University of Basel, MCR (Meteorology, Climatology and Remote Sensing) in the city of Basel. A 18 m tall tower is mounted on the flat roof top of a 20 m high building (BKLI) since 2003. The neighbourhood of the site is mainly characterised by the highly trafficked inner ring road Klingelbergstrasse to the east, oriented along the 200°/20° axis, as well as by residential buildings enclosing green backyards, to the west. Furthermore, some tall university buildings are located approximately 250 m to the north and the northeast of the site. An overview of the study site, including the average footprint estimation is given in fig. 1. A more detailed description of the site characteristics is given in Lietzke and Vogt (2013).

*Fig. 1: Aerial image (Geodaten Kanton Basel-Stadt 2015) of the BKLI site. The map shows a segment of 2x2 km centered on BKLI. The white grid lines indicate steps of 200 m. Additionally the average footprint estimation is shown. Thick solid and dashed black lines indicate the 90 % and 50% contour respectively. Thin dashed black lines give additional information on the contour shape in steps of 10 %. Radial black dashed lines indicate sectors of 45° used during investigation. Sectors are numbered clockwise from 1 to 8, starting at the northern sector.*

## 3. Material and Methods

### I. Measurements and data processing

The EC system of the BKLI site, operative since May 2004 is the central part of this study. The instruments are mounted to a vertical extension at the tower top at a total height of 39 m above street level. According to Lietzke

and Vogt (2013) and Feigenwinter et al. (2012) the measurements take place above the roughness sublayer (RSL), but inside the urban inertial sublayer (ISL). The EC system consists of an ultrasonic anemometer (GILL HS, hereinafter called sonic) and an open path $CO_2/H_2O$ analyser (LI-7500), both facing northwards (20°), allowing the predominant winds (fig. 2) from east and west to pass the measuring volume mostly undisturbed. Data are processed following the guidelines of Aubinet et al. (2012), complemented by experiences from visual data inspection. Overall data availability after completion of post-processing is approximately 70% for flux data and up to 98% for other meteorological quantities.

**II. Gap filling**

Gaps in flux data are filled by a gap-filling algorithm which is based on look-up tables (LUT). For this study an improved, moving LUT (mLUT) technique (Reichstein et al. (2005)) is implemented. Instead of LUTs based on static bins for distinct temporal and meteorological conditions, the gap-filling values are derived from a moving frame. Data availability after gap-filling is approximately 98%.

**III. Flux upscaling**

Fluxes measured by the EC method always represent an integrated signal from all sources and sinks within the footprint area. If these sources and sinks are not equally distributed around the station, the derived fluxes and thus, the final NEE, highly depend on the relative frequency of occurrence of wind sectors with distinct source/sink characteristics. Thus, due to non-normal frequency distribution of wind direction, some sectors may be over- or underestimated, which may prevent to capture representative fluxes for the heterogeneous land use around the station.

Lietzke et al. (2015) introduced a method for the calculation of a so-called expected net ecosystem exchange (eNEE) or expected flux ($eF_c$). The method accounts for heterogeneous source/sink distribution by weighting sectorial fluxes with the relative frequency of occurrence of each wind sector. For this study, the methodology was slightly adapted, by using mLUT instead of static LUT. To achieve expected values, from each sector a time series is generated and then gaps are filled solely with corresponding sectorial data by mLUT. The sectorial time series are then averaged arithmetically for each point in time, which results in the average expected flux or eNEE, respectively.

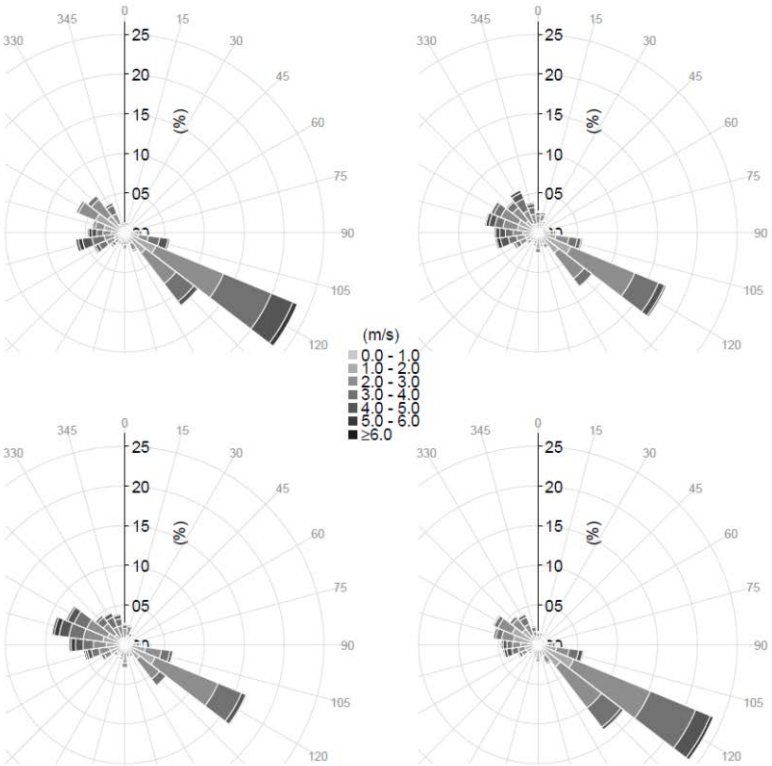


*Fig 2.: Relative frequencies of wind direction (24 bins) and velocities at BKLI for winter (a), spring (b), summer (c) and autumn (d).*

## 4. Results

### I. The role of unequal frequency distribution of wind direction for the interpretation of $CO_2$ measurements (flux upscaling)

As a consequence of the frequency distribution anomaly (FDA) of wind direction, sectorial statistics, particularly totals (e.g. NEE), cannot be interpreted straightforward. The necessity of applying a weighting factor becomes clear, when fig. 3a is taken into account. The overall average yearly NEE for BKLI is 4.14 kgC $m^{-2}$ $y^{-1}$. Due to the unequal distribution of sources and wind direction 1.61 kgC $m^{-2}$ $y^{-1}$ can be attributed to sector 4. Emissions from the other sectors vary between 0.20 and 0.52 kgC $m^{-2}$ $y^{-1}$. Sector 4 is clearly overestimated because of the conjunction of high $CO_2$ emissions from the Klingelbergstrasse to the east as well as the high frequency of occurrence of this wind direction. In contrast sectors 3 and 7 nearly reach the same NEE, the first being influenced by high emissions from traffic and the latter just occurring frequently but normally showing low $F_C$ values.

Fig. 3b shows the eNEE after removal of FDA influences. As one would expect from the land use classification sectors 2-5 are linked to the highest eNEE values, due to strong $CO_2$ emissions from traffic. Sector 5 clearly peaks out of the others (0.95 kgC $m^{-2}$ $y^{-1}$), because it is facing exactly along the Klingelbergstrasse. Thus this sector covers the largest absolute area of major road class and for this reason captures the most $CO_2$. In contrast sectors 3 and 4 (0.66 and 0.73 kgC $m^{-2}$ $y^{-1}$) cover only a relatively small fraction of major road, but the vicinity of the source seems to compensate for this effect, which is why they also show relatively high values. Sectors 1 and 7-8 show the smallest values, because no major sources of $CO_2$ can be found within the footprint area. On average upscaling of $F_C$ to $eF_C$ leads to an increase of the resulting yearly NEE of up to 10%.

*a)* *b)*

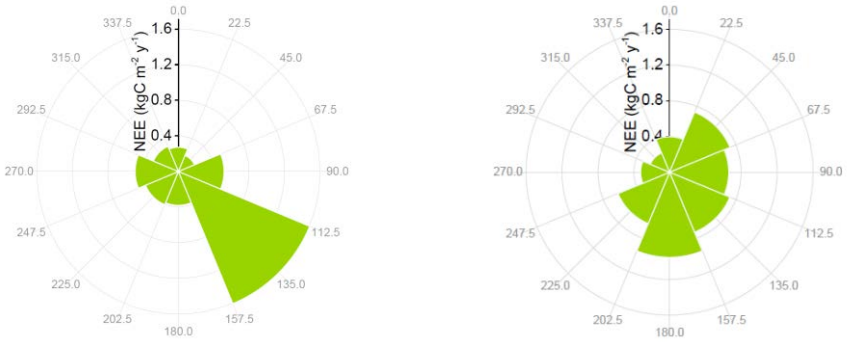


*Fig. 3: Average yearly NEE (a) and eNEE (b) for each sector from 2004-2014. Sector definition according to fig. 1.*

### II. Long term time series of urban $CO_2$ concentration

To the $CO_2$ concentration data a 90-day running mean filter was applied (fig. 4a). Like this singular events (e.g. short periods of low/high temperature, abnormal emissions) are smoothed out and the seasonal growth and decline of $\rho_c$ can be better visualised. Generally the shape of the seasonal cycles is similar from year to year with a sinusoid pattern. Increase of $\rho_c$ in autumn and decrease in spring happens relatively fast, whereas in winter and summer there is always a short period of nearly steady $\rho_c$. The seasonal amplitude, defined as the difference between the average DJF value and the following average JJA value is on average 21.2 ppm, but varies between 16.8 ppm in 2005 and 26.2 ppm in 2006. Except for single years with abnormal high (DJF in 2006 and 2014) or low (JJA in 2007 and 2008) peak values of absolute $\rho_c$, the inter-annual variability in seasonality is relatively small. Wintertime maxima start at 405.1 ppm in 2005 and grow up to 426.8 ppm in early 2014, whereas during same time period the minima increase from 378.9 to 402.2 ppm. With an average year-to-year growth rate of 3.0 ppm $y^{-1}$ the mean annual $CO_2$ concentration raised from 385.8 to 415.9 ppm, which is a plus of 30.1 ppm over the last decade. The slope of the linear regression calculated over the whole time period is 1.97 ppm $y^{-1}$. This is very similar to Hernández-Paniagua et al. (2015) who reports 2.5 ppm $y^{-1}$ from analysis of 10 years of measurements at the Royal Holloway University nearby London and 1.9 ppm $y^{-1}$ from measurements at Mace Head Atmospheric Research Station on the west coast of Ireland. Additionally these results also compare well to the global trend of 2.0 ppm $y^{-1}$ between 2001 and 2013 as published in the last IPCC report (IPCC 2013) calculated from Mauna Loa and South Pole data.

In addition to the local $\rho_c$, Fig. 4a also shows $\rho_c$ of nearby background concentration measurements, carried out at Schauinsland (SAL, 40 km northwards, 1205 m asl (Luftmessnetz des Umweltbundesamtes 2015)) and Jungfraujoch (JFJ, 120 km southwards, 3580 m asl (University of Bern 2015)). Clearly, the seasonality of both stations is very similar to BKLI, but the seasonal amplitude is much smaller at SAL and JFJ. Long term trends of background concentration are comparable to BKLI, with 2.04 ppm $y^{-1}$ at SAL and 1.90 ppm $y^{-1}$ at JFJ. Differences can be observed concerning the time of peak values. Obviously the background concentration responds with some time lag to the increase and decrease of $\rho_c$ during winter and summer, respectively. On average BKLI

peaks in December, whereas SAL is behind by 2 month (February) and JFJ by 3 month (March). The delay in time of seasonal peaks is most likely a function of distance from sources and/or height above ground. This becomes more evident, if the IQR is considered in Fig. 4a. As expected, the variability is much larger at BKLI, followed by SAL and JFJ. It has to be mentioned, that the different variability is also subject to different measurement principles at the three stations, with BKLI being the only EC site with open-path gas analyzer. Nevertheless, the data clearly shows, that the local and background concentration are coupled by a hysteresis. They are both subject to the same seasonal variation and long term trend, whereas the amplitude and the peak date are controlled by the vicinity of $CO_2$ sources. During winter the coupling is delayed by up to 3 month, which is most likely due to more frequent high inversions, and generally more stable conditions. This prohibits an efficient and direct exchange between boundary layer air masses and the free atmosphere. In contrast, during summer the atmosphere is well mixed by large vertical convective dynamics and the coupling between local and background concentration is more direct.

*a)*

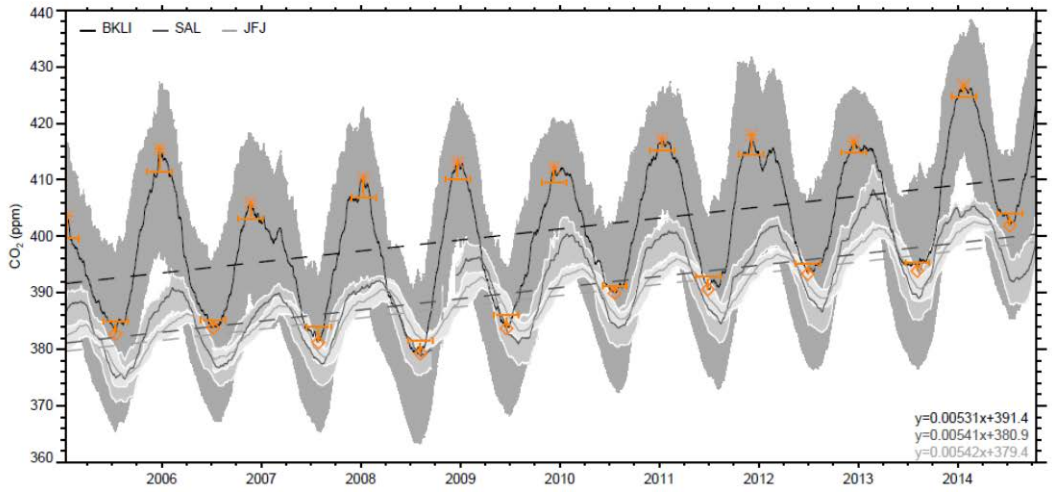


*b)*

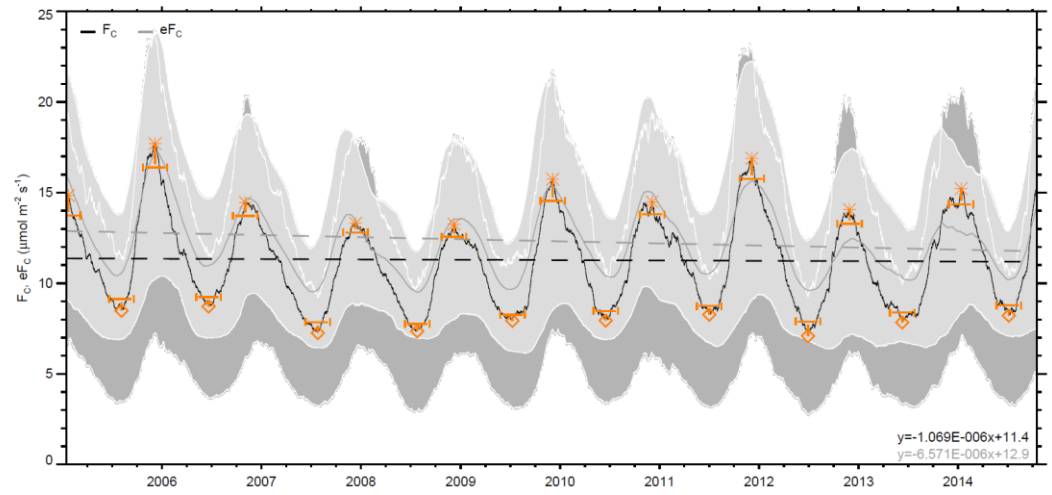


*Fig. 4: (a) Time series of $CO_2$ concentration at BKLI (dark grey), Schauinsland (medium grey) and Jungfraujoch (light grey), (b) and time series of $F_C$ (dark grey) and $eF_C$ (light grey). Solid lines are 90 days running means of half hourly data. IQR of each time series are indicated by grey shaded areas, outlined by white lines. Dashed lines show the linear regression for each time series. Additionally, average seasonal values of each DJF and JJA season (orange horizontal bars), winter maxima (asterisk) and summer minima (diamonds) are drawn.*

**III. Long term time series of urban $CO_2$ flux**

In Fig. 4b a 90 days running mean filter was applied to $F_C$ and $eF_C$, respectively. Generally $F_C$ follows a sinusoid pattern with maximum values between 13.25 and 17.7 µmol $m^{-2}$ $s^{-1}$ during winter and minimum values between 7.1 and 8.7 µmol $m^{-2}$ $s^{-1}$ during summer. Despite, $F_C$ shows large variability on daily basis, the seasonal pattern is well defined and only few secondary peaks (e.g. winter 2013/2014) occur. The IQR as a measure for the scatter of $F_C$ is larger with maximum values of 17.3 µmol $m^{-2}$ $s^{-1}$ during winter compared to 6.0 µmol $m^{-2}$ $s^{-1}$ during the

summer month. The IQR as well as the minimum and maximum values indicate, that the year-to-year minima vary less ($\sigma$=0.54 µmol $m^{-2}$ $s^{-1}$) than the maxima values ($\sigma$=1.53 µmol $m^{-2}$ $s^{-1}$). Interestingly, the variability is only weakly represented by the lower quartile, whereas the upper quartile follows well the inter-annual differences both during winter and summer. Average $F_C$ does only rarely come below a stable threshold value around 3-4 µmol $m^{-2}$ $s^{-1}$ in summer and 6-7 µmol $m^{-2}$ $s^{-1}$ in winter. Most likely this represents the well mixed background flux of the local urban metabolism, which is slightly higher during the winter month, when more sources (heating) and less sinks (vegetation) are active. In addition, from the minimum values it becomes clear, that even during the vegetated period $CO_2$ uptake by photosynthesis is not able to compensate for the emission. This is also observed in most other comparable urban environments and only results from vegetated suburban neighbourhoods report clear offsetting effects by vegetation (Bergeron and Strachan 2011; Crawford et al. 2011; Ramamurthy and Pardyjak 2011; Velasco et al. 2013).

In contrast to $\rho_c$ no clear long term trend is visible for $F_C$. Between 2005 and 2009 $F_C$ clearly shows a declining tendency, but this period is followed by three years of slightly higher fluxes. Over the last ten years $F_C$ is reduced only by -0.2 µmol $m^{-2}$ $s^{-1}$, whereas the trend for $eF_C$ is somewhat larger with -1.2 µmol $m^{-2}$ $s^{-1}$. Even though the trend points towards the expected direction, it is surprisingly low. Analysis of the nearby traffic count data shows, that after the opening of the northern traffic bypass in 2007/2008, total traffic volume was reduced by approximately 25 % during the following years. By comparison, $F_C$ was reduced by 1.6 % and $eF_C$ by 8.9%, respectively. Even though the reduction in traffic volume seems to have a reducing effect on $F_C$, the correlation is relatively weak (not shown). This is in contrast to the very strong relations achieved by regression analysis of diurnal cycles of $F_C$ and traffic. The question then arises, as to how far a single nearby traffic count is representative for the investigation area. From the current data, it seems like the shape of the diurnal cycle of $F_C$ is given by the increase and decrease of the traffic volume, but the transport processes between the street canyon and the above inertial sublayer might be more sophisticated.

## 5. Conclusions

During the last decade a large number of studies presenting carbon dioxide flux measurements over a wide range of different urban environments have been released, as EC systems became an affordable and reliable tool. Among a couple of multi-year studies we are the first presenting a full decade of urban $CO_2$ flux measurements, which offers the opportunity to investigate seasonality and long term trends of $CO_2$ with a reliable and solid data set. Assuredly, during the following years, more time series of sufficient length (10+ years) will be available, undoubtedly increasing the focus of research on investigation of inter-annual variability and long-term trend analysis. Such datasets represent not only a chance to learn more about the complex pathways of greenhouse gas emissions and the “metabolism” of the heterogeneous urban landscape, but also poses new challenges such as the proper implementation of gap filling strategies, the assessment of trends and the validation of models as well.

### *References*

Aubinet, M., T. Vesala, and D. Papale, 2012: Eddy covariance, a practical guide to measurement and data analysis. *Springer Atmospheric Sciences*, **Ed. 1**, 1-438.

Reichstein, M., and Coauthors, 2005: On the separation of net ecosystem exchange into assimilation and ecosystem respiration: review and improved algorithm. *Global Change Biology*, **11,** 1424-1439.

Lietzke, B., and R. Vogt, 2013: Variability of CO2 concentrations and fluxes in and above an urban street canyon. *Atmospheric Environment*, **74**, 60-72.

Feigenwinter, C., R. Vogt, and A. Christen, 2012: Eddy Covariance Measurements Over Urban Areas. 377-397. In: Aubinet, M., T. Vesala, and D. Papale, 2012: Eddy covariance: a practical guide to measurement and data analysis. *Springer Atmospheric Sciences*, **Ed. 1**, 1-438.

Lietzke, B., R. Vogt, C. Feigenwinter, and E. Parlow, 2015: On the controlling factors for the variability of carbon dioxide flux in a heterogeneous urban environment. *International Journal of Climatology*.

Hernández-Paniagua, I. Y., and Coauthors, 2015: Diurnal, seasonal, and annual trends in atmospheric CO2 at southwest London during 2000–2012: Wind sector analysis and comparison with Mace Head, Ireland. *Atmospheric Environment*, **105,** 138-147.

Bergeron, O., and I. B. Strachan, 2011: CO2 sources and sinks in urban and suburban areas of a northern mid-latitude city. *Atmospheric Environment*, **45,** 1564-1573.

Crawford, B., C. S. B. Grimmond, and A. Christen, 2011: Five years of carbon dioxide fluxes measurements in a highly vegetated suburban area. *Atmospheric Environment*, **45,** 896-905.

Ramamurthy, P., and E. R. Pardyjak, 2011: Toward understanding the behavior of carbon dioxide and surface energy fluxes in the urbanized semi-arid Salt Lake Valley, Utah, USA. *Atmospheric Environment*, **45,** 73-84.

Velasco, E., M. Roth, S. H. Tan, M. Quak, S. D. A. Nabarro, and L. Norford, 2013: The role of vegetation in the CO2 flux from a tropical urban neighbourhood. *Atmospheric Chemistry and Physics*, **13,** 10185-10202.